Diagn Interv Radiol 2019; 25:416–420

ABDOMINAL IMAGING

ORIGINAL ARTICLE

Hyperintensity at fat spared area in steatotic liver on the hepatobiliary phase MRI

Emre Ünal
İlkay Sedakat İdilman
Ali Devrim Karaosmanoğlu
Mustafa Nasuh Özmen
Deniz Akata
Muşturay Karcaaltıncaba

PURPOSE
We aimed to investigate the reasons for hyperintensity at fat spared area in steatotic liver at hepatobiliary phase (HBP) on gadolinium-ethoxybenzyl-diethylenetriamine pentaacetic acid (Gd-EOB-DTPA) enhanced liver magnetic resonance imaging.

METHODS
Twenty-two patients with focal fat spared area demonstrating hyperintensity on HBP images were included. A region of interest was placed on in- and opposed-phase images at fat spared area and liver to measure the fat. The measurement was also performed on precontrast T1-weighted and HBP images. The signal intensities of spleen, kidney, muscle, intervertebral disc, and spinal cord were also recorded.

RESULTS
The mean fat fraction of liver and fat spared area was 24.86% (8%–46%) and 8.41% (1%–34%), respectively ($P < 0.001$). There was a significant positive correlation between liver parenchyma fat fraction and delta fat fraction (r=0.74, $P < 0.001$). The mean signal intensity values of fat spared areas were higher compared with liver on precontrast T1-weighted and HBP images ($P < 0.001$). The mean relative enhancement ratio of liver and fat spared areas were 0.98 (0.05–1.90) and 1.15 (0.22–2.03), respectively ($P < 0.001$). However, in 6 patients, the relative enhancement ratio of liver and fat spared areas were almost equal. The uptake of Gd-EOB at fat spared area was not correlated with the degree of steatosis (r = -0.01, $P = 0.95$).

CONCLUSION
Fat spared area in steatotic liver appears hyperintense on HBP images due to increased relative enhancement ratio and/or baseline hyperintensity on precontrast images.

Liver steatosis may induce various imaging appearances and some of these changes may cause confusion particularly in cancer patients (1–4). Previous studies have demonstrated the value of magnetic resonance imaging (MRI) over computed tomography (CT) and ultrasonography (US) in the evaluation of fatty liver (5–7). Fat spared areas, hypersteatotis, and patchy areas of fat infiltration can be easily diagnosed by in- and opposed-phase images. Although these changes could be easily identified by liver MRI, the metabolic effect of steatosis on liver may cause confusion on positron emission tomography-computed tomography (PET-CT) scans (8, 9).

It is known that liver steatosis may induce liver fibrosis and decreased parenchymal function in chronic and severe cases. Impaired liver function is a serious complication; however, it could be recognized on the hepatobiliary phase of gadolinium-ethoxybenzyl-diethylenetriamine pentaacetic acid (Gd-EOB-DTPA) enhanced liver MRI, as areas of decreased contrast enhancement due to reduced number or function of hepatocytes (10, 11). Nevertheless fat spared areas in the liver may induce increased signal intensity on HBP images due to preserved or even increased parenchymal function (12, 13). Preserved liver function in these areas could be inadvertently reported as a metastasis on PET-CT images due to increased fluorodeoxyglucose (FDG) uptake compared with suppressed steatotic background liver (8, 9).

From the Department of Radiology (M.K. ✉ *musturayk@yahoo.com*), Hacettepe University School of Medicine, Ankara, Turkey.

Received 05 December 2018; revision requested 29 December 2018; last revision received 04 March 2019; accepted 16 April 2019.

Published online 8 August 2019.

DOI 10.5152/dir.2019.18535

You may cite this article as: Ünal E, İdilman İS, Karaosmanoğlu AD, Özmen MN, Akata D, Karcaaltıncaba M. Hyperintensity at fat spared area in steatotic liver on the hepatobiliary phase MRI. Diagn Interv Radiol 2019; 25:416–420.

Signal intensity characteristics of fat spared areas on liver MRI in patients who received Gd-EOB-DTPA have not been previously analyzed. Therefore, we aimed to investigate the reasons of hyperintensity at fat spared area on hepatobiliary phase of Gd-EOB-DTPA enhanced liver MRI.

Methods

Study population

A total of 22 consecutive patients with a focal fat spared area demonstrating increased signal intensity on Gd-EOB-DTPA enhanced liver MRI were included in the study (Fig. 1). This was a retrospective analysis of a database prospectively collected between 2014 and 2017. This retrospective study has been approved by the local ethics committee. Informed consent was waived.

MRI examinations

The MRI examinations were performed on a 1.5T HDxt MRI system (GE Healthcare). An 8-channel phased array body coil was used for MRI acquisitions. The patients were examined in the supine position. Gadoxetate disodium (Primovist, Bayer Schering Pharma) was injected intravenously at a dose of 0.025 mmol/kg. A three-dimensional gradient-echo (LAVA) sequence was used for dynamic liver examination. Consequently, the hepatobiliary phase images were obtained 20 minutes after the contrast material injection.

Image processing

The acquired images were analyzed on PACS station (GE Healthcare). An elliptic (~1 cm^2) region of interest (ROI) was placed on in- and opposed-phase images at focal fat spared area and background steatotic liver parenchyma by avoiding major vessels and bile ducts to measure the fat fraction. The measurement was also performed on precontrast fat suppressed T1-weighted and hepatobiliary phase images, while maintaining the same section plane for fat spared area and liver parenchyma. The signal intensities (SI) of spleen, kidney, erector spinae muscle, intervertebral disc, and spinal cord on precontrast fat-suppressed T1-weighted and hepatobiliary phase images were also recorded.

The fat fraction was calculated for the liver parenchyma and fat spared area according to the following formula: Fat fraction= In phase SI – opposed phase SI / 2× In phase SI (14). The difference of fat fraction between liver parenchyma and fat spared area was defined as delta fat fraction. The relative enhancement ratio for the liver parenchyma and fat spared area was calculated with the following equation: (HBP-SI) – (Precontrast-SI) / (Precontrast-SI).

The intensity ratios were measured for both the liver parenchyma and fat spared area with the following equation: (HBP-SI of liver or fat spared area / HBP-SI of other body part) / (Precontrast-SI of liver or fat spared area / Precontrast-SI of other body part) (15, 16). The measurements were made by a single radiologist who had 8 years of experience in reading liver MRI examinations.

Statistical analysis

All statistical analyses were performed using descriptive summaries. Means and standard deviations or median and range were computed for all continuous data. The Kolmogorov-Smirnov test was used to test the normal distribution of variables. Comparison between two groups in terms of continuous variables was assessed by repeated measures ANOVA, paired Student t-test or Wilcoxon signed rank test, where applicable.

The degree of association between continuous variables was calculated by Pearson test. For all tests, a two-tailed *P* value of <0.05 was considered statistically significant.

Results

In all patients (11 men, 11 women), focal fat spared area appeared hyperintense at

Main points

- Liver steatosis may induce liver fibrosis and decrease parenchymal function.
- Impaired liver function could be recognized on the hepatobiliary phase of Gd-EOB-DTPA enhanced liver MRI, as areas of decreased contrast enhancement due to reduced number or function of hepatocytes.
- Fat spared areas in the liver may induce increased signal intensity on HBP images due to preserved or even increased parenchymal function.
- Increased or preserved parenchymal function at fat spared area could be a potential pitfall for false positive PET-CT due to relatively increased metabolic activity.

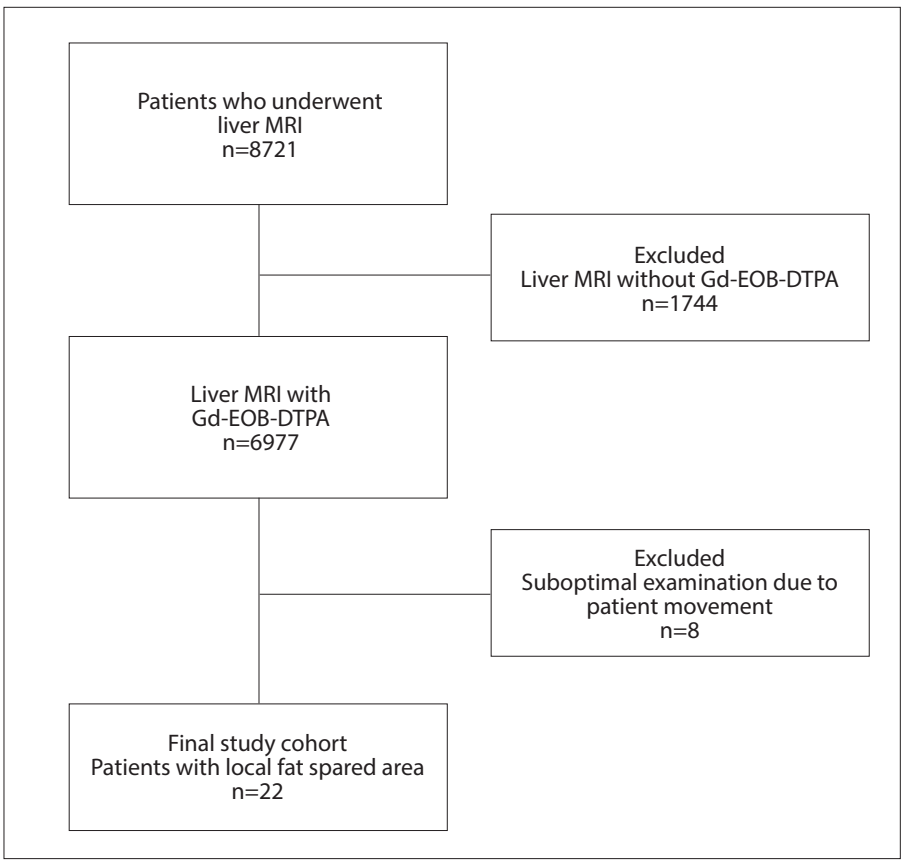

Figure 1. The flow chart of patient selection.

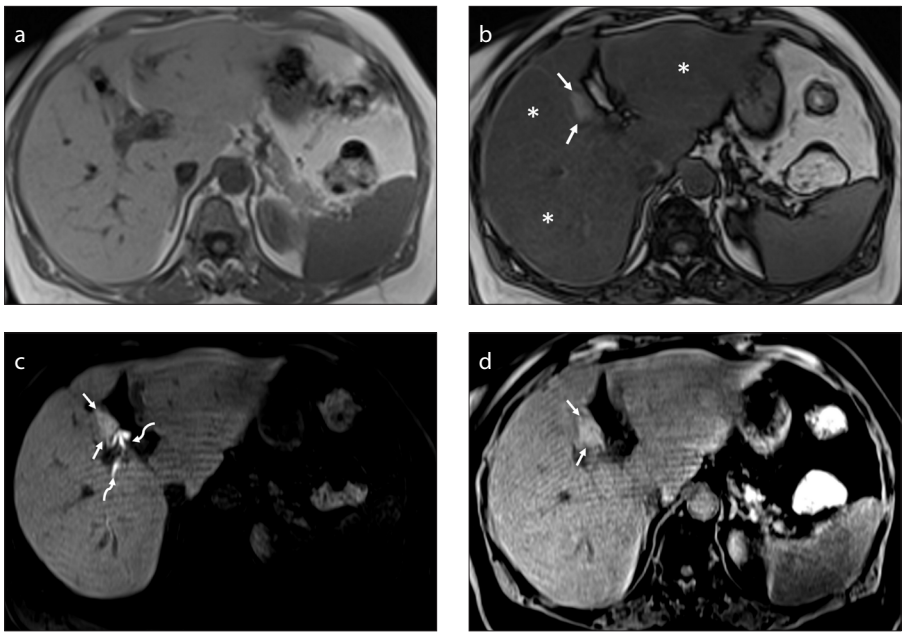

Figure 2. a–d. A 60-year-old woman with gallbladder carcinoma underwent Gd-EOB-DTPA enhanced liver MRI due to nonspecific nodular lesions detected on ultrasonography. In-phase **(a)** and opposed-phase **(b)** images demonstrate marked liver steatosis (fat fraction of 26%) identified with decreased signal intensity on opposed phase image (**b,** *asterisks)*. A fat spared area (fat fraction of 2.7%) located anterior to main portal vein is recognized with preserved high signal intensity on opposed-phase image (**b,** *arrows*). Increased signal intensity on hepatobiliary phase image **(c)** indicates hyperfunctioning hepatocytes *(arrows)* at fat spared area. The relative enhancement ratio was 0.79 which was more than that of the rest of the liver (ratio of 0.54). Contrast filled bile ducts due to excretion of hepatobiliary-specific contrast agent are also seen *(curved arrows)*. Note preserved signal intensity of fat spared area *(arrows)* compared with steatotic liver on precontrast fat suppressed T1-weighted image **(d)**.

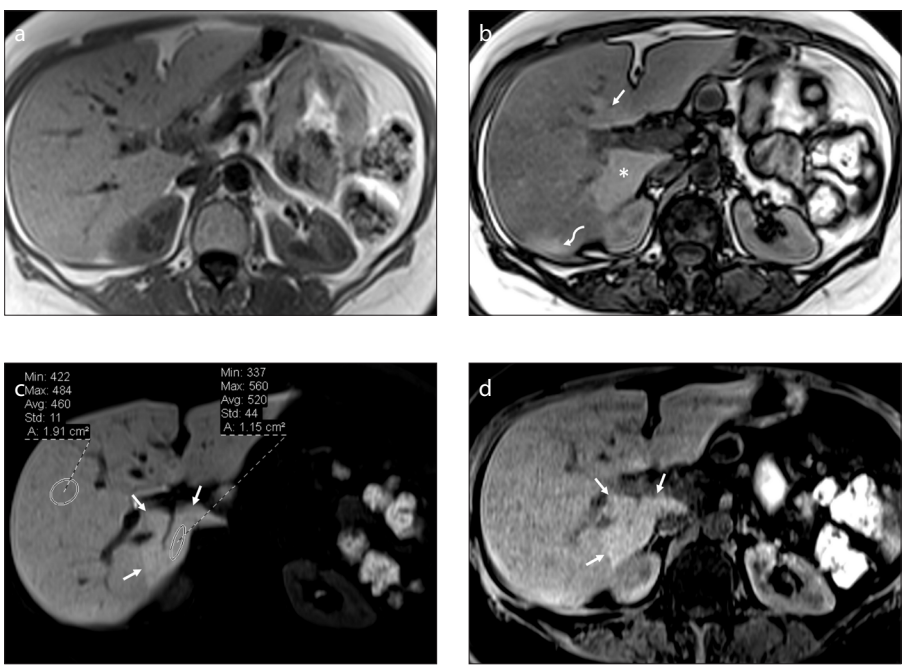

Figure 3. a–d. A 52-year-old woman underwent Gd-EOB-DTPA enhanced liver MRI due to elevated liver enzymes within a short period of time. In-phase **(a)** and opposed-phase **(b)** images demonstrate inhomogeneous liver steatosis (fat fraction of 23%) with several fat spared areas located anterior to main portal vein **(b,** *arrow)*, caudate lobe *(asterisk)*, and subcapsular region of segment 7 of the liver *(curved arrow)*. Increased signal intensity on hepatobiliary phase image **(c)** indicates hyperfunction (**c,** *arrows*) at fat spared area (fat fraction of 1%). The relative enhancement ratio was 1.4 which was more than that of the rest of the liver (ratio of 1.1). Preserved signal intensity of fat spared area (**d,** *arrows*) on precontrast fat suppressed T1- weighted image **(d)** is also noted.

hepatobiliary phase of liver MRI (Figs. 2, 3). The mean age of the participants was 49.9 years (range, 18–70 years). There was no patient with liver cirrhosis or elevated liver enzymes in our study. There was no signal alteration in fat spared areas on T2-weighted and diffusion-weighted images, indicating absence of focal nodular hyperplasia, adenoma or hemangioma.

Focal fat spared area was present at segment 4 (n=16), caudate lobe (n=4), adjacent to gallbladder (n=1), and subcapsular liver parenchyma (n=1). The mean fat fraction of the liver and fat spared areas was 24.86% (range, 8%–46%) and 8.41% (range, 1%–34%), respectively. There was a statistically significant difference between fat fraction of the liver and fat spared areas ($P < 0.001$, paired t-test). The mean signal intensity of liver and fat spared areas on precontrast fat-suppressed T1-weighted images was 330 (range, 78–890) and 405 (range, 105–904) with statistically significant difference ($P < 0.001$, paired Student t-test). The mean signal intensity of liver and fat spared areas on hepatobiliary phase images was 602 (range, 208–1436) and 799 (range, 319–1957) ($P < 0.001$, paired Student t-test). The mean relative enhancement ratio of liver and fat spared areas was 0.98 (range, 0.05–1.90) and 1.15 (range, 0.22–2.03), respectively ($P < 0.001$, paired Student t-test). However, in 6 out of 22 patients, the mean relative enhancement ratios of liver (1.11) and fat spared areas (1.13) were almost equal (slightly increased at fat spared area) (Fig. 4).

The mean delta fat fraction was 16.55% (range, 4.7%–38.9%). There was a significant and positive correlation between liver parenchyma fat fraction and delta fat fraction (r=0.74, $P < 0.001$, Pearson test) (Fig. 5). There was no statistically significant correlation between fat fraction of liver or fat spared areas and the signal intensities of both parameters before contrast (r=-0.01, $P = 0.96$, and r=-0.01, $P = 0.53$, respectively, Pearson test), after contrast (r=0.06, $P = 0.78$, and r=-0.01, $P = 0.55$, respectively, Pearson test), and in terms of relative enhancement ratio (r=0.18, $P = 0.42$, and r=-0.01, $P = 0.95$, respectively, Pearson test).

The median liver to muscle and fat spared areas to muscle intensity ratio was 2.05 (range, 1.67–3.98) and 2.25 (range, 2–4), respectively ($P = 0.048$, Wilcoxon signed rank test). The median liver to spinal cord and fat spared areas to spinal cord intensity ratio

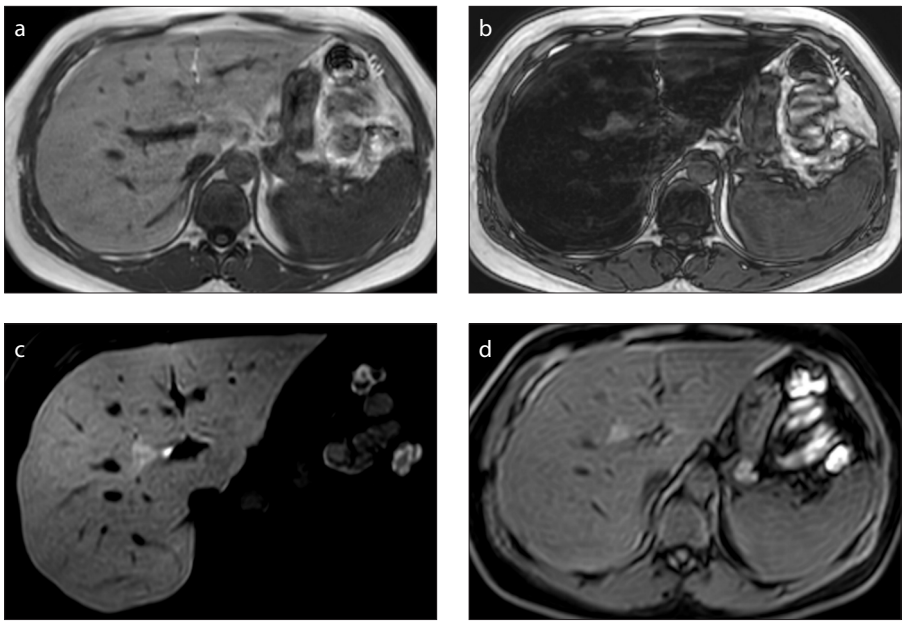

Figure 4. a–d. A 45-year-old man with significant liver steatosis. In-phase **(a)** and opposed-phase **(b)** images demonstrate liver steatosis (fat fraction of 35%) and fat spared area (fat fraction of 19%) located anterior to main portal vein. The hyperintensity at focal fat spared area on hepatobiliary phase image **(c)** was due to influence of existing hyperintensity on precontrast T1-weighted image **(d)**. The relative enhancement ratio difference between liver parenchyma (0.222) and focal fat spared area (0.227) was negligible.

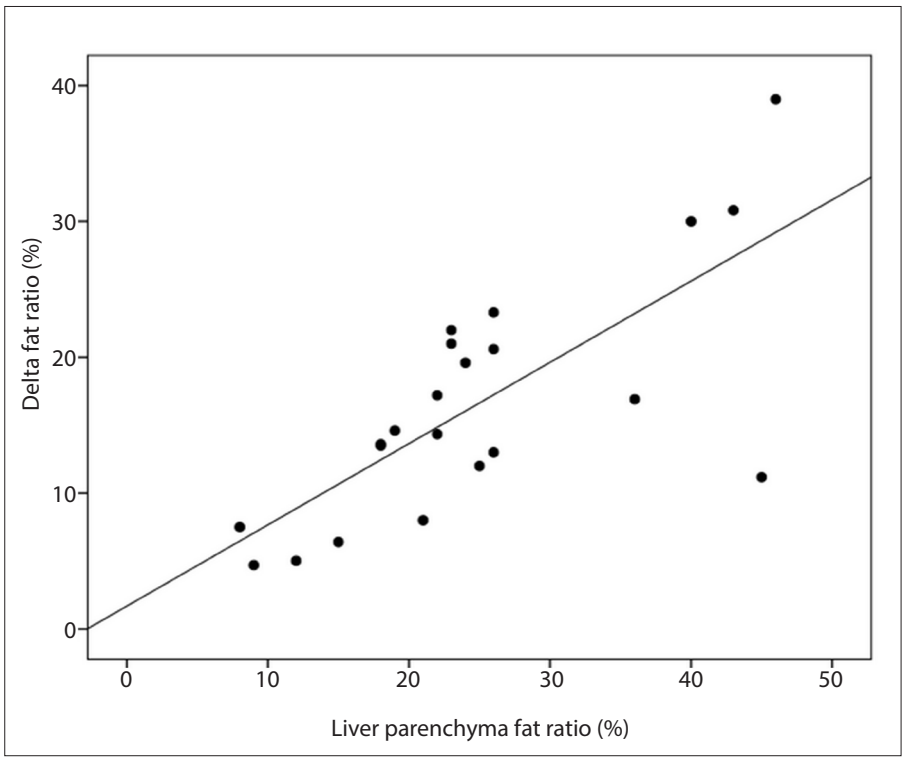

Figure 5. Scatterplot shows the correlation between hepatic steatosis and delta hepatic fat fraction (r=0.741, $P < 0.001$).

was 2.34 (range, 0–3) and 2.47 (range, 0–4), respectively ($P = 0.034$, Wilcoxon signed rank test). The median liver to spleen and fat spared areas to spleen intensity ratio was 1.78 (range, 1–3) and 1.87 (range, 1–3), respectively ($P = 0.18$, Wilcoxon signed rank test). The median liver to intervertebral disc and fat spared areas to intervertebral disc intensity ratio was 2.14 (range, 1–4) and 2.24 (range, 1–5), respectively ($P = 0.21$, Wilcoxon signed rank test).

Discussion

Focal fat spared areas in a steatotic liver can demonstrate increased signal intensity on HBP images. We found relatively increased function in fat spared areas (mean relative enhancement ratio of 1.15) compared with background liver (mean relative enhancement ratio of 0.98, $P < 0.001$). In the studies evaluating the effectiveness of Gd-EOB-DTPA enhanced MRI in differentiation of normal liver from the fibrotic or cirrhotic livers, authors reported higher enhancement ratios and signal intensity values on HBP images in normal livers or in low stage of liver fibrosis compared with severe fibrotic livers (11, 17–20). In addition, steatohepatitis has also been reported to induce decreased parenchymal intensity related to fibrosis state as a consequence of hepatocyte dysfunction (11, 21). Based on our results, we suggest that fat spared area demonstrating hyperintensity on HBP images may contain hyperfunctioning hepatocytes compared with background liver. Therefore fat spared area may exhibit more hyperintensity compared with steatotic liver parenchyma on HBP images. However, we cannot rule out the effect of fibrosis level differences between fat spared area and rest of liver parenchyma due to lack of histopathologic examination in our study. Nevertheless, we observed a significant and positive correlation between the liver parenchyma fat fraction and delta fat fraction (r=0.775, $P < 0.001$), which indicates that higher fat accumulation in the liver increases the gap between fat fraction of fat spared area and background liver parenchyma.

Liver steatosis may induce various imaging appearances particularly on CT and US (1–4, 22). Liver MRI could be used as a problem solving tool in the assessment of focal liver lesions detected in a steatotic liver by CT and US. However, great attention should be given to assessment of PET-CT scan in a steatotic liver. Focal areas of fat infiltration could be misinterpreted as metastases on CT or US; however, focal fat does not usually cause confusion on PET-CT scans because these areas are usually not hypermetabolic. We demonstrated higher signal intensity in focal fat spared areas on hepatobiliary phase images can be due to relatively increased hepatocyte function or basal hyper-

intensity on precontrast T1-weighted MRI. Hyperintense appearing focal fat spared areas in patients with relatively increased function are potential pitfalls for false positive PET-CT scans (8, 9). We also found that these areas exhibit increased signal intensity values on precontrast fat suppressed T1-weighted images as a consequence of suppressed signal of background steatotic liver on a fat suppressed sequence and in 6 patients relative enhancement ratio difference was negligible. Therefore, a focal fat spared area should not be interpreted as a space occupying liver lesion due to T1 shortening effect on precontrast fat suppressed T1-weighted image. Focal nodular hyperplasia may also result in hyperintensity on hepatobiliary phase images; however, lack of contrast enhancement on dynamic postcontrast sequences may enable differentiation of FNH from fat spared area.

In the literature, various MRI-derived indices obtained by measuring the signal intensity of liver and other organs on HBP images, were investigated for predicting liver fibrosis stage or to differentiate normal liver from cirrhosis (16, 23–26). Nojiri et al. (16) reported that the best correlation between MRI and the liver biopsy was achieved with liver to-intervertebral disc ratio, followed by relative liver enhancement and with liver-to-spleen ratio being the least accurate for discriminating liver fibrosis. Kukuk et al. (23) concluded that liver to spleen contrast ratio and relative liver enhancement were significantly correlated with liver function tests. Moreover, Kumazawa et al. (24) reported that the intensity ratio of the enhanced liver to spinal cord was the most suitable method among other MRI-derived indices to predict liver fibrosis. In our study, relative enhancement ratio and signal intensity values on hepatobiliary phase images demonstrated statistically significant difference between fat spared area and steatotic liver. We could not find statistically significant correlation between fat fraction of liver or fat spared areas and relative enhancement ratio. This may be due to lack of patients with cirrhosis or severely fibrotic liver in our study.

Our study had several limitations that should be addressed. First, it was a retrospective analysis. Second, the number of study cohort was small. Third, fibrosis level difference between fat spared areas and liver parenchyma was not histopathologically confirmed. Fourth, FDG-PET-CT scans of the patients were not obtained. Therefore, we cannot conclude, but may suggest that fat spared area in a steatotic liver could be responsible for false positive PET-CT results, due to increased relative enhancement ratio which reflects hyperfunctioning liver parenchyma.

In conclusion, focal fat spared area can appear hyperintense on hepatobiliary phase MRI due to two reasons: (*i*) influence of existing hyperintensity on precontrast T1-weighted images, (*ii*) relatively increased parenchymal enhancement (function). The latter might be a potential pitfall for false positive PET-CT due to relatively increased metabolic activity.

Conflict of interest disclosure

The authors declared no conflicts of interest.

References

1. Basaran C, Karcaaltincaba M, Akata D, et al. Fat-containing lesions of the liver: cross-sectional imaging findings with emphasis on MRI. AJR Am J Roentgenol 2005; 184:1103–1110. [CrossRef]
2. Idilman IS, Ozdeniz I, Karcaaltincaba M. Hepatic steatosis: etiology, patterns, and quantification. Semin Ultrasound CT MR 2016; 37:501–510. [CrossRef]
3. Jang JK, Jang HJ, Kim JS, Kim TK. Focal fat deposition in the liver: diagnostic challenges on imaging. Abdom Radiol (NY) 2017; 42:1667–1678. [CrossRef]
4. Unal E, Karaosmanoglu AD, Akata D, Ozmen MN, Karcaaltincaba M. Invisible fat on CT: making it visible by MRI. Diagn Interv Radiol 2016; 22:133–140. [CrossRef]
5. Kakihara D, Nishie A, Harada N, et al. Performance of gadoxetic acid-enhanced MRI for detecting hepatocellular carcinoma in recipients of living-related-liver-transplantation: comparison with dynamic multidetector row computed tomography and angiography-assisted computed tomography. J Magn Reson Imaging 2014; 40:1112–1120. [CrossRef]
6. Muhi A, Ichikawa T, Motosugi U, et al. Diagnosis of colorectal hepatic metastases: comparison of contrast-enhanced CT, contrast-enhanced US, superparamagnetic iron oxide-enhanced MRI, and gadoxetic acid-enhanced MRI. J Magn Reson Imaging 2011; 34:326–335. [CrossRef]
7. Park VY, Choi JY, Chung YE, et al. Dynamic enhancement pattern of HCC smaller than 3 cm in diameter on gadoxetic acid-enhanced MRI: comparison with multiphasic MDCT. Liver Int 2014; 34:1593–1602. [CrossRef]
8. Harisankar CN. Focal fat sparing of the liver: a nonmalignant cause of focal FDG uptake on FDG PET/CT. Clin Nucl Med 2014; 39:e359-361.
9. Purandare NC, Rangarajan V, Rajnish A, Shah S, Arora A, Pathak S. Focal fat spared area in the liver masquerading as hepatic metastasis on F-18 FDG PET imaging. Clin Nucl Med 2008; 33:802–805. [CrossRef]
10. Feier D, Balassy C, Bastati N, Stift J, Badea R, Ba-Ssalamah A. Liver fibrosis: histopathologic and biochemical influences on diagnostic efficacy of hepatobiliary contrast-enhanced MR imaging in staging. Radiology 2013; 269:460–468. [CrossRef]
11. Wu Z, Matsui O, Kitao A, et al. Usefulness of Gd-EOB-DTPA-enhanced MR imaging in the evaluation of simple steatosis and nonalcoholic steatohepatitis. J Magn Reson Imaging 2013; 37:1137–1143. [CrossRef]
12. Unal E, Akata D, Karcaaltincaba M. Liver Function Assessment by Magnetic Resonance Imaging. Semin Ultrasound CT MR 2016; 37:549–560. [CrossRef]
13. Campos JT, Sirlin CB, Choi JY. Focal hepatic lesions in Gd-EOB-DTPA enhanced MRI: the atlas. Insights Imaging 2012; 3:451–474. [CrossRef]
14. Reeder SB, Cruite I, Hamilton G, Sirlin CB. Quantitative assessment of liver fat with magnetic resonance imaging and spectroscopy. J Magn Reson Imaging 2011; 34:729–749. [CrossRef]
15. Nojiri S, Fujiwara K, Shinkai N, Endo M, Joh T. Evaluation of hepatocellular carcinoma development in patients with chronic hepatitis C by EOB-MRI. World J Hepatol 2014; 6:930–938. [CrossRef]
16. Nojiri S, Kusakabe A, Fujiwara K, et al. Noninvasive evaluation of hepatic fibrosis in hepatitis C virus-infected patients using ethoxybenzyl-magnetic resonance imaging. J Gastroenterol Hepatol 2013; 28:1032–1039. [CrossRef]
17. Kim HY, Choi JY, Park CH, et al. Clinical factors predictive of insufficient liver enhancement on the hepatocyte-phase of Gd-EOB-DTPA-enhanced magnetic resonance imaging in patients with liver cirrhosis. J Gastroenterol 2013; 48:1180–1187. [CrossRef]
18. Tamada T, Ito K, Higaki A, et al. Gd-EOB-DTPA-enhanced MR imaging: evaluation of hepatic enhancement effects in normal and cirrhotic livers. Eur J Radiol 2011; 80:e311–316. [CrossRef]
19. Tsuda N, Okada M, Murakami T. New proposal for the staging of nonalcoholic steatohepatitis: evaluation of liver fibrosis on Gd-EOB-DTPA-enhanced MRI. Eur J Radiol 2010; 73:137–142. [CrossRef]
20. Nilsson H, Blomqvist L, Douglas L, et al. Gd-EOB-DTPA-enhanced MRI for the assessment of liver function and volume in liver cirrhosis. Br J Radiol 2013; 86:20120653. [CrossRef]
21. Yamada T, Obata A, Kashiwagi Y, et al. Gd-EOB-DTPA-enhanced-MR imaging in the inflammation stage of nonalcoholic steatohepatitis (NASH) in mice. Magn Reson Imaging 2016; 34:724–729. [CrossRef]
22. Tom WW, Yeh BM, Cheng JC, Qayyum A, Joe B, Coakley FV. Hepatic pseudotumor due to nodular fatty sparing: the diagnostic role of opposed-phase MRI. AJR Am J Roentgenol 2004; 183:721–724. [CrossRef]
23. Kukuk GM, Schaefer SG, Fimmers R, et al. Hepatobiliary magnetic resonance imaging in patients with liver disease: correlation of liver enhancement with biochemical liver function tests. Eur Radiol 2014; 24:2482–2490. [CrossRef]
24. Kumazawa K, Edamoto Y, Yanase M, Nakayama T. Liver analysis using gadolinium-ethoxybenzyl-diethylenetriamine pentaacetic acid-enhanced magnetic resonance imaging: Correlation with histological grading and quantitative liver evaluation prior to hepatectomy. Hepatol Res 2012; 42:1081–1088. [CrossRef]
25. Motosugi U, Ichikawa T, Sou H, et al. Liver parenchymal enhancement of hepatocyte-phase images in Gd-EOB-DTPA-enhanced MR imaging: which biological markers of the liver function affect the enhancement? J Magn Reson Imaging 2009; 30:1042–1046. [CrossRef]
26. Yoneyama T, Fukukura Y, Kamimura K, et al. Efficacy of liver parenchymal enhancement and liver volume to standard liver volume ratio on Gd-EOB-DTPA-enhanced MRI for estimation of liver function. Eur Radiol 2014; 24:857–865. [CrossRef]